Thermophotovoltaic Generation with Microstructured Tungsten Selective Emitters

doi: 10.1063/1.1841896

Thermophotovoltaic Generation with Microstructured Tungsten Selective Emitters

Hitoshi Sai[ab], Takahiro Kamikawa[a], Yoshiaki Kanamori[a], Kazuhiro Hane[a], Hiroo Yugami[a], and Masafumi Yamaguchi[b]

[a] *Graduate school of Engineering, Tohoku University, Aoba 01, Aramaki, Aoba-ku, Sendai, 980-8579 JAPAN*
[b] *Toyota Technological Institute, Hisakata 2-12-1, Tempaku-ku, Nagoya, 468-8511 JAPAN*

Abstract. To accomplish a good spectral matching between an emitter and photovoltaic cells, two-dimensional surface-relief gratings with a period of 1.0 – 1.2 μm composed of rectangular microcavities were fabricated on single crystalline W substrates as a selective emitter for thermophotovoltaic generation. The emitters displayed strong emission in the near infrared region where narrow-bandgap photovoltaic cells could efficiently convert photons into electricity. The enhancement of thermal emission was attributed to the microcavity effect. Thermophotovoltaic generation tests were carried out with different kinds of emitters. The W gratings showed more than two-times higher generation efficiency when compared to a SiC emitter. Optical constants of W at high temperatures were investigated by ellipsometry, and it was shown that spectral emissivity of the emitters depended on their temperatures especially in the infrared region.

INTRODUCTION

In thermophotovoltaic (TPV) systems, thermal radiation from a high-temperature body (emitter) is converted into electricity with photovoltaic (PV) cells. A key issue to develop high-performance TPV generators is the spectral matching between the emitter's thermal radiation and the PV cell's spectral response which is usually ranged from the visible (VIS) to the near infrared (NIR) regions. For this purpose, spectrally selective emitters, whose emissivity is high only in the PV cell's sensitive region and low outside it, have been researched by many researchers [1]. Most of the previous reports on selective emitters concern rare-earth elements such as Er and Ho which have strong emission bands intrinsically.

Recently, it has been demonstrated by several groups that the spectral feature of thermal radiation can be controlled by surface gratings or photonic crystals [2-7]. They have utilized several interactions between thermal radiation and modulated surfaces such as surface plasmon polaritons [2,3], surface phonon polaritons [4], microcavity effect [5,6], and photonic bandgaps [7]. This technique is very attractive for thermal systems in which thermal radiation plays an important role like TPV generation. Our group has reported that two-dimensional (2D) tungsten (W) gratings composed of microcavities can behave as selective emitters due to the cut-off effect of micro-cavities [6].

CP738, *Thermophotovoltaic Generation of Electricity, Sixth Conference*
edited by A. Gopinath, T.J. Coutts, and J. Luther

Microstructured selective emitters have potential advantages such as adjustability of spectral design and adaptability to various materials, and therefore the further progress is expected. However, to our knowledge, most of the previous reports concern with only spectral features and there are few reports on practical applications. In this study, TPV generation tests are carried out with microstructured W selective emitters with different structural parameters to demonstrate their contribution for high-efficiency and high-power TPV systems.

MICROSTRUCTURED TUNGSTEN SELECTIVE EMITTERS

Spectral Design by Numerical Simulation

Maruyama et al. proposed that peak wavelengths on thermal emission spectra from metallic microcavities with an aperture are given by the relation [5]

$$\lambda_{lmn} = \frac{2}{\sqrt{\left(l/L_x\right)^2 + \left(m/L_y\right)^2 + \left(n/2L_z\right)^2}} \qquad (1)$$

where l, m and n are integers (l, m = 0, 1, 2, … and n = 0, 1, 3, 5, …) and $L_x \times L_y \times L_z$ denotes the size of microcavities. At most one of the integers can be zero. The maximum value of λ_{lmn} is called the cut-off wavelength, λ_c. Photons with wavelengths of $\lambda > \lambda_c$ cannot exist inside microcavities. If one forms a microcavity array on a metallic surface, then it is expected that the thermal radiation is enhanced only in the range of $\lambda < \lambda_c$. A good selective emitter will be realized by choosing λ_c corresponding to the bandgap wavelength of PV cells.

Equation (1) tells which wavelengths can be existed inside a microcavity, but it does not tell how much energy is distributed to each wavelength. Therefore, we investigated the spectral properties of microstructured selective emitters by numerical simulation based on rigorous coupled-wave analysis (RCWA) method [8]. The optical constants (n, k) of W reported in the literature [9] were used in the calculations. We calculated the spectral absorptivity α_λ of various W gratings and suppose it equal to their emissivity ε_λ according to Kirchhoff's law.

Figure 1 shows the calculated α_λ of several microstructured W emitters. In this study, calculation models are restricted into 2D surface-relief gratings composed of rectangular microcavities as depicted in the inset with the following geometrical parameters: grating period Λ, aperture size a, grating depth d, polar angle θ, azimuthal angle ϕ and polarization angle ψ. In the case that the aspect ratio (d/a) is substantially smaller than unity, a sharp peak is observed on the spectrum. This peak probably originated from the coupling of surface waves supported by the grating and electromagnetic waves, since the peak wavelength is almost the same as Λ. This kind of peak is too narrow for TPV applications. On the other hand, for the gratings with larger d/a, multiple peaks appear on the spectra. They show high α_λ (~ ε_λ) almost in

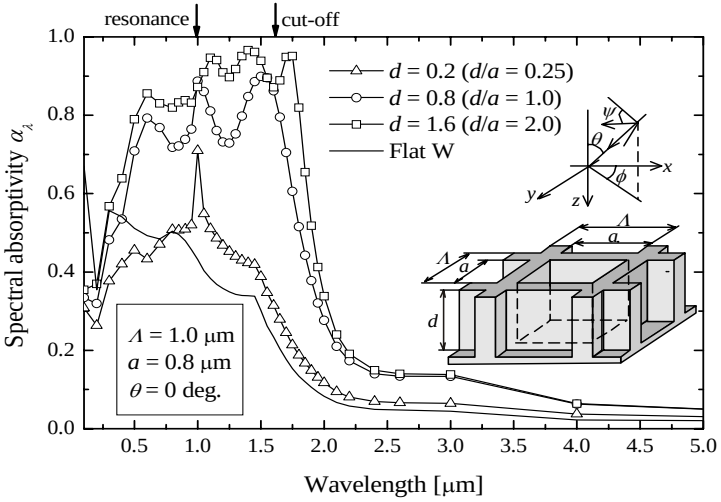

FIGURE 1. Calculated spectral absorptivity α_λ of 2D W surface gratings with Λ = 1.0 μm and a = 0.8 μm for ϕ = 0° and ψ = 45°. The calculation model is schematically drawn in the inset.

the range of $\lambda < \lambda_c$, and therefore it is expected that this α_λ enhancement is mainly due to the microcavity effect. It has been already indicated that the microcavity effect is not so sensitive to the angles of emission, which is a preferable characteristic for TPV [6].

Sample Fabrication

2D surface gratings were fabricated by means of the electron beam (EB) lithography and fast atom beam etching techniques described in the previous report [6]. In this study, we fabricated the three gratings with different parameters on single crystalline W substrates. The structural parameters of the samples are listed in Table 1 and a scanning electron micrograph of Sample C is shown in Fig. 2 with their spectral properties. λ_c of our samples is ranged from 1.6 to 1.9 μm, and hence emissivity increase is expected in that region.

It is possible to estimate ε_λ of non-transparent materials like metals from spectral reflectivity ρ_λ based on Kirchhoff's law. Before measuring ε_λ, ρ_λ of the samples were

TABLE 1. Structural parameters of the fabricated W gratings.

Sample	Λ[μm]	a [μm]	d [μm]
A	1.0	0.8	0.7
B	1.2	0.9	0.63
C	1.2	0.95	0.78

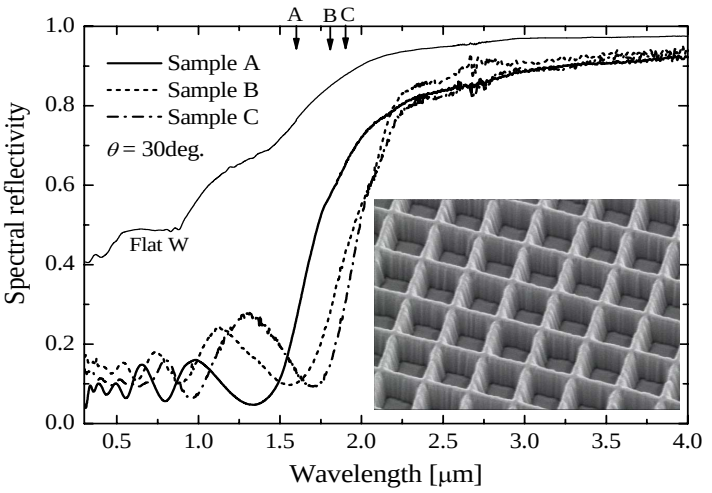

FIGURE 2. Spectral reflectivity ρ_λ of the W gratings and a flat W at $\theta = 30°$ measured with a diffuse reflection geometry and the randamly polarized incident beam at room temperature. The downward arrows denote λ_c of the three gratings. A SEM image of Sample C is shown in the inset.

measured with a diffuse reflection geometry (PIKE, easidiff). The incident angle was set to 30°. As plotted in Fig.2, ρ_λ of all the gratings decreases sabstantially in $\lambda < 2.0$ μm keeping high ρ_λ at longer wavelengths. Multiple local minima are also observed on the spectra, and they shift with deepening or widening microcavities. This reveals that those reflectivity minima are originated from the microcavity effect.

Experimental Setup

A schematic diagram of the emission measurement system used in this study is drawn in Fig. 3. Samples are heated up to 1400K by an electric heater with a sapphire window. Because of the small area of the grating region, thermal radiation from the samples is expanded and focused by a CaF_2 lens on a pinhole to shut out stray light. After that, the radiation is collimated by another CaF_2 lens and analyzed by a Fourier transform infrared spectrometer (FT-IR) (Perkin Elmer, GX2000). During heating, Ar gas containing 5% H_2 is passed through the heater casing to prevent oxidation. Sample temperature T is measured with a radiation thermometer. In the case of W gratings whose ε_λ is unknown, T is determined by measuring T of the flat part around the grating. For TPV generation tests, we use an InGaAs photodiode (Hamamatsu photonics K.K., G8370-03) with the sensitive region of 0.9 – 1.7 μm and the size of ϕ = 0.3 mm as a TPV cell. It is attached to a movable stage located just behind the

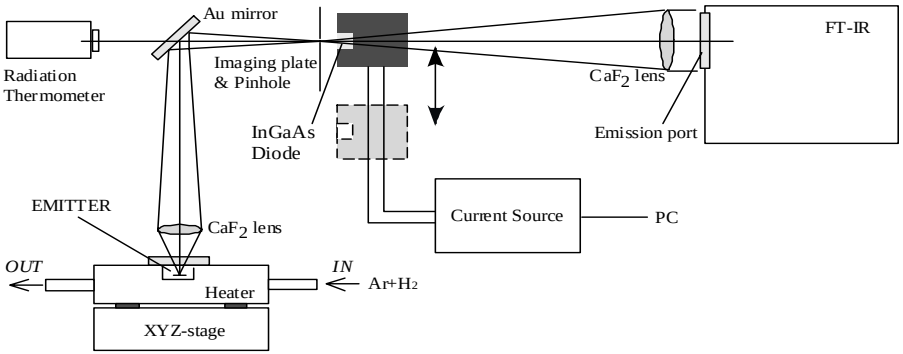

FIGURE 3. A schematic of the apparatus for emission measurement and TPV demonstration.

pinhole. After measuring emission spectra, the InGaAs diode is inserted in the optical path and I-V characteristics are measured.

Spectral Emissivity and TPV Generation Demonstration

Figure 4 shows ε_λ of the samples measured at high T. ε_λ of all the samples increases drastically in $\lambda < 2.0$ μm. Clear emission peaks are observed on the spectra at 1.22 μm for Sample A, at 1.48 μm for Sample B and at 1.56 μm for Sample C. These spectral properties correspond to those of the ρ_λ shown in Fig. 2, but the peak positions slightly shifted to the shorter wavelength. A maximum emissivity over 0.8 is obtained for all the samples. These results showed that the W gratings behave as spectrally selective emitters for TPV applications and can control their spectral feature by adjusting the cavity shape. On the other hand, the measured ε_λ in the infrared region is somewhat higher than that expected from the ρ_λ shown in Fig. 2. This is probably explained by the T-dependence of the optical constants of W.

Figure 5 (A) shows the maximum output power P_{max} obtained by TPV generation tests as functions of T. Sufficiently large fill factor over 0.7 was observed for all data, while only small P_{max} (μW ~ mW) was obtained mainly due to the small area of the photo diode and emitters, and the large distance between them. For all emitters, P_{max} increases rapidly with increasing T since the total emissive power is generally proportional to T^4. Sample B gives larger P_{max} than a flat W emitter because of its higher emissivity in the NIR region. However, SiC, which is a typical broad-band emitter with the emissivity of 0.9, gives the maximum P_{max} among the three emitters at a constant temperature.

At high T over 1000K, thermal radiation is dominant as compared with thermal conduction and convection. Thereby it can be supposed that the input thermal energy to heat an emitter is approximately proportional to the emissive energy from its surface. In Fig. 5(B), P_{max} is re-plotted as a function of the total emissive power incident on the diode, EP_{total}. Sample B reaches higher T and gives much larger P_{max}

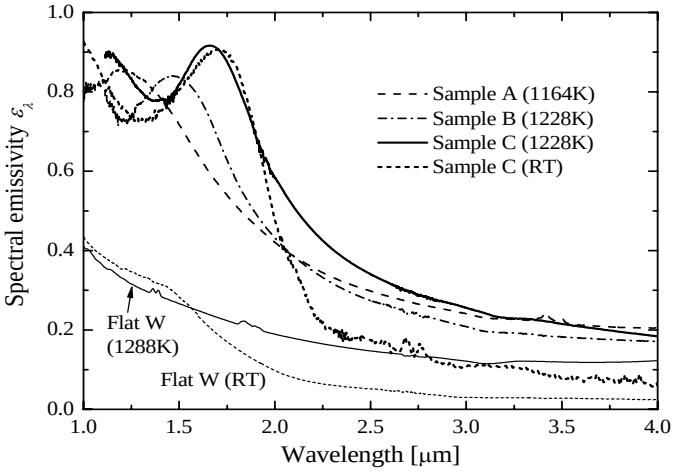

FIGURE 4. Spectral emissivity ε_λ of the W gratings and a flat W at the normal direction.

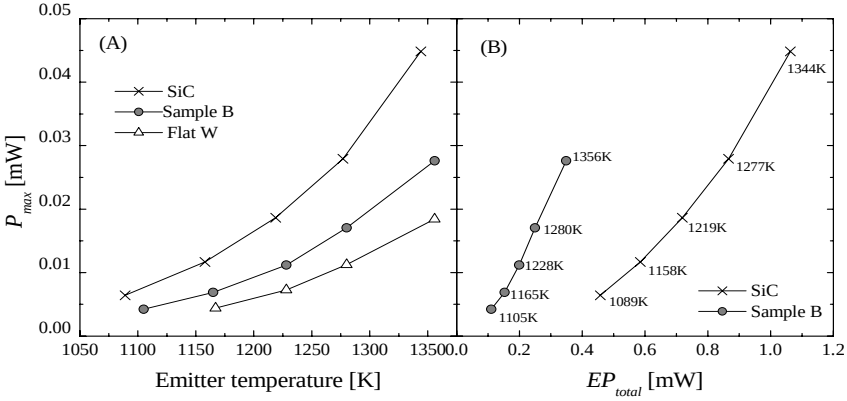

FIGURE 5. (A) P_{max} of the InGaAs photo diode radiated by several emitters as functions of emitter temperatures. **(B)** P_{max} of the InGaAs photo diode radiated by several emitters as functions of the total incident emissive power, EP_{total}.

than SiC at constant EP_{total} because of its spectral selectivity. The ratio of P_{max} to EP_{total}, namely, the slope in Fig. 5(B) gives a relative evaluation of the conversion efficiency from the input energy to electricity. The figure shows that Sample B will achieve more than two-times the efficiency of SiC.

Sample B emits about 20 kW/m^2 in λ = 0.9 – 1.7 μm at 1400K. Assuming the emitter-to-cell view factor of 0.7 and PV cell's efficiency of 0.5 in that region, we can

develop a 100W TPV generator with microstructured W emitters with the area of 140 cm^2. The area is reduced to 110 cm^2 for the same system with a SiC emitter, but it needs about three-time larger input energy to keep the same *T*. In other words, W gratings can provide higher *T* and larger output power under the same input energy. Therefore it is concluded that microstructured W emitters provides TPV generators with both a high-efficiency and high power density.

OPTICAL CONSTANTS AT HIGH TEMPERATURES

As previously mentioned, ε_λ of the W emitters depends on their *T* especially in the IR region. This should be considered in numerical simulations to determine the emitter design. However there have been few reports on the *T*-dependence of (*n*, *k*) or permittivity. In this study, we attempt to measure (*n*, *k*) of W at high-temperatures by ellipsometry.

Figure 6 shows a schematic drawing of the high-temperature ellipsometry system used in this study. This system can measure (*n*, *k*) from λ = 0.4 to 2.2 μm. A mechanically polished W sheet with the size of 25 × 25 mm^2 was prepared as a specimen. It was heated in a vacuum atmosphere to prevent oxidation during measurement.

The measured (*n*, *k*) of flat W at several *T* is plotted in Fig. 7 (A). It is clearly observed that W's (*n*, *k*) depends on *T* especially in the IR region, where W behaves as a nearly ideal metal. *n* increases and *k* decreases with increasing *T* there. However, both *n* and *k* are almost invariant in the VIS region.

Suppose that W is a perfectly non-transparent material, α_λ or ε_λ is determined with (*n*, *k*) by the following relation:

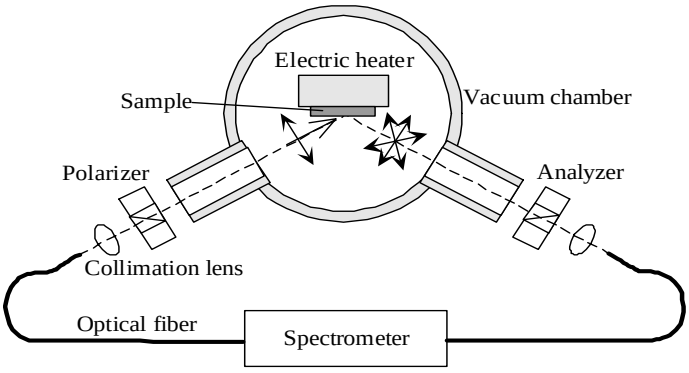

FIGURE 6. A schematic diagram of the high-temperature spectral ellipsometory system.

$$\alpha_\lambda = \varepsilon_\lambda = 1 - \frac{(n-1)^2 + k^2}{(n+1)^2 + k^2} \qquad (2)$$

According to this equation, a small change in k will cause a significant alternation in α_λ or ε_λ because W has much larger k than n in the IR region.

Next we conducted RCWA simulations on 2D binary W gratings as shown in Fig. 1 with measured (n, k). The result is shown in Fig. 7 (B). The calculated α_λ increased particularly in the IR region with increasing T. This tendency is consistent with the measured data plotted in Fig. 4. From these results, it was revealed that T-dependence of (n, k) must be considered to design and evaluate microstructured selective emitters.

Based on Drude theory, increasing T causes the reduction of the electron life time τ in metals, and this results in the increase of ε_λ [10]. It is also expected that reducing τ increases the skin depth of metals. In this situation, the confinement modes in microcavities will spread across a large wavelength range. Taking these matters into consideration, it is expected that spectral properties of the W gratings as a spectrally selective device are somewhat suppressed at high T.

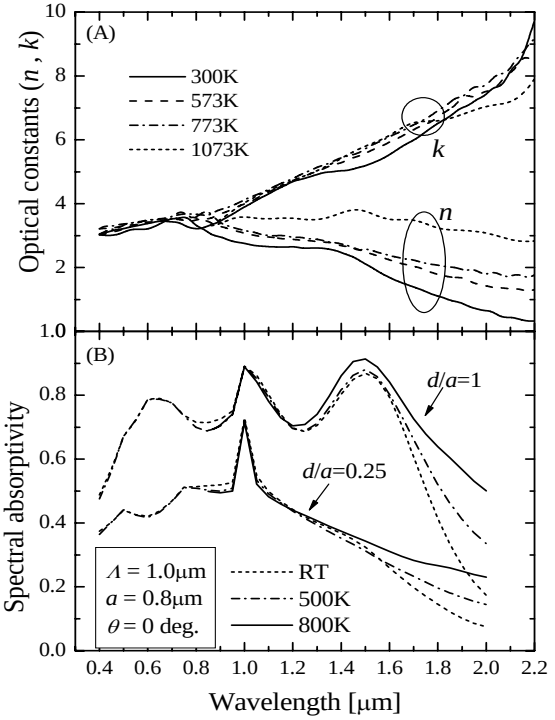

FIGURE 7. (A) Measured optical constants (n, k) of flat W. **(B)** Spectral absorptivity α_λ of the W gratings with Λ=1.0μm, a=0.8 μm calculated by RCWA using (n, k) at high temperatures.

SUMMARY

The spectral properties of W were successfully controlled based on the microcavity effect introduced by 2D W surface gratings composed of microcavities. This result shows that the spectral feature of microstructured selective emitters can be varied according to the bandgap of TPV cells. It is confirmed experimentally that the W selective emitters have advantages for high-power and high-efficiency TPV systems. The studies on fabrication processes for a large area device will be the next target. From this point of view, it is considered that 2D surface gratings are more suitable than 3D photonic crystals [7].

Optical constants of tungsten at high temperatures were measured by means of ellipsometry. It was confirmed that their temperature dependence affects on tungsten's spectral features particularly in the IR region and in our case it aggravates the performance of microstructured W selective emitters. This result suggests that the temperature dependence of the spectral properties must be considered to design and evaluate microstructured selective emitters.

ACKNOWLEDGMENTS

The authors would like to appreciate the support of the Ministry of Education, Science, Sports and Culture, Japan. The authors are also grateful for the technical support of the Venture Business Laboratory in Tohoku University.

REFERENCES

1. Licciulli, A., Diso, D., Torsello, G. Tundo, S., Maffezzoli, A., Lomascolo, M., and Mazzer, M., *Semicond. Sci. Technol.* **18** S174- S186 (2003).
2. Heinzel, A., Boerner, V., Gombert, A., Bläsi, B., Wittwer, V., and Luther, J., *J. Mod. Opt.* **47** 2399-2419 (2001).
3. Kusunoki, F., Takahara, J., and Kobayasi, T., *Electron. Lett.* **39** 23-24 (2003).
4. Greffet, J.-J., Carminati, R., Joulian, K., Mulet, J.-P., Mainguy, S., and Chen, Y., *Nature* **416** 61-64 (2002).
5. Maruyama, S., Kashiwa, T., Yugami, H., and Esashi, E., *Appl. Phys. Lett.* **79** 1393-1395 (2001).
6. Sai, H., Kanamori, Y., and Yugami, H., *Appl. Phys. Lett.* **82** 1685-1687 (2003).
7. Lin, S.Y., Fleming, J.G., and El-Kady, I., *Opt. Lett.* **28** 1909-1911 (2003).
8. Moharam, M.G., Proceedings of SPIE **883** 8-10 (1988).
9. Lynch, D.W. and Hunter, W.R., *Handbook of Optical Constants of Solids I*, edited by Palik, E.D., New York: Academic Press, 1985, pp. 334-341.
10. Ujihara, K., *J. Appl. Phys*. **43** 2376-2383 (1972).